Unsupervised Methods for Fly Sperm Motility Analysis

John Thomson[1] **Jinman Park**[2] **Veronika Magdanz**[3] **David Clausi**[2]
[1] Electrical and Computer Engineering, University of Waterloo
[2] Vision and Image Processing Lab, Systems Design Engineering, University of Waterloo
[3] Medical Microrobotics Lab, Systems Design Engineering, University of Waterloo
{jwthomson,jinman.park,veronika.magdanz,dclausi}@uwaterloo.ca

Abstract

Standard methods of sperm cell motility analysis involve the tracking of single cells and determining overall motility and velocity of the cells. For *Drosophila*, an important model organism for reproduction and genetic studies, such methods cannot be applied due to the large size and entanglement of the sperm cells, which makes single cell motion challenging with current video analysis methods. We propose two metrics which can be used to numerically quantify this motility. To evaluate the efficacy of these metrics, a synthetic data set and accompanying ground truth metrics are developed.

1 Introduction

Spermatozoa are the most diverse cell types, expressed by a vast variety of cell shapes and sizes [1]. Quantifying sperm motility is one of the most important methods to predict sperm quality and fertilization outcome, besides sperm morphology and total sperm number. In most mammalian sperm, the motility can easily be measured based on the forward motion of sperm and characterized by single cell velocity and overall percentage of motility. The fruit fly *Drosophila melanogaster* has become an important model organism to study reproduction and effects of environmental and genetic modifications on the off-spring, thanks to its fast reproduction rate [2]. Especially for studying reproduction and sexual selection, *Drosophila melanogaster* has many advantages, such as fast generation time, large number of offspring, possible in vivo imaging and a decoded genome since 2000. *Drosophila melanogaster* is also very useful for studying speciation, sperm competition and the evolution of male and female reproductive traits [2].

The evaluation of sperm motility in *Drosophila melanogaster* has been challenging due to the extremely long cells of over a millimeter, their bundling behaviour and rather crawling motion, which makes the measurement of forward motion of single cells impossible. In previous studies, it was found that drosophila sperm move in circular patterns in the uterus using arc-line waveforms. It was also visible that they enter the seminal receptacle in parallel tail-leading formations by transforming from circular to linear waveforms[3]. Highspeed videomicroscopy allows the recording of *Drosophila melanogaster* sperm motion, but its quantification has not been achieved up to now. We present here a motility benchmark of multiple unsupervised motion tracking methods such as optical flow and temporal variation for the analysis of drosophila sperm motion. We compare the outcome of these methods on a new synthetic data set that we generate to mimic the visual behaviour of drosophila sperm motion by defining a new metric for motility. We give implications on the sensitivity and overall suitability of this method to be applied to sperm cell analysis of species in which single cell tracking is impossible. The goal of our approach is to quantify the overall level of sperm motility, rather than extracting data for the beat frequency or amplitude of single cells.

2 Methods

We present two different approaches to quantifying drosophila sperm motility based on 1) temporal variation of video recordings of drosophila sperm motion, and 2) optical flow. Videos of free drosophila sperm released from the seminal vesicle are recorded in phase contrast mode in order to provide a sharp image contrast (see Figure 1). Sperm flagella appear white while the background is black. Sperm motion will thus cause a movement of the bright pixels. Both optical flow and temporal variation are used to quantify the fluctuations

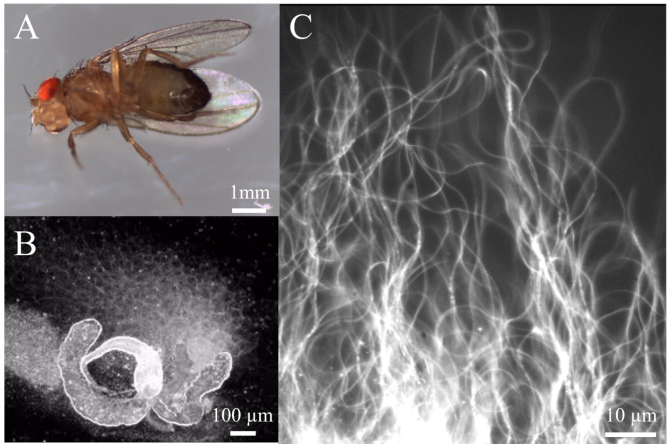

Fig. 1: Spermatozoa of the fruit fly. A) Model organism *Drosophila melanogaster*. B) Microscopic image of the seminal vesicle that is releasing sperm cells onto a cover slide. C) 400x magnification of spermatozoa. Sperm cells appear white on dark background in phase contrast microscopy.

created by motion of sperm in the image sequence as a single scalar value. To evaluate the accuracy and robustness of these metrics, a synthetic data set of 500 videos with varying motility are generated. Various methods of quantifying the ground truth motility of the videos are proposed, and each analysis method is evaluated against these ground truth metrics.

2.1 Videomicroscopy of *Drosophila melanogaster* Spermatozoa

Dissection of the seminal vesicle was performed under a stereoscope in a 5 microliter droplet of phosphate buffered saline. The seminal vesicle was transferred onto a fresh 20 microliter droplet on a new slide and covered with a cover slide. Videomicroscopy was performed immediately after dissection with a Leica DSM inverted microscope and a Phantom highspeed camera, recording videos at 50 frames per second (FPS) in phase contrast and 100-400x magnification.

2.2 Metrics for Motility

2.2.1 Optical Flow

Motility analysis of videos with optical flow uses Farneback's algorithm [4], implemented in OpenCV. Optical flow is applied to all pixels in all pairs of subsequent frames. The magnitude of the motion at every pixel in all frames is averaged to obtain a single metric for motility. Applying this method, motility can be expressed as:

$$M = \sum_{i=1}^{f-1} \sum_{j=1}^{h} \sum_{k=1}^{w} V_{ijk} \tag{1}$$

where f is the total number of frames, w is the width of the video frame, h is the height of the video frame, and V_{ijk} is the magnitude of the velocity calculated via optical flow between the i-th and $(i+1)$-th frames at the pixel located at the j-th row of the k-th column, with indexes beginning at the top left. Optical flow tends to be less accurate when cells are grouped close together. The individual cells become

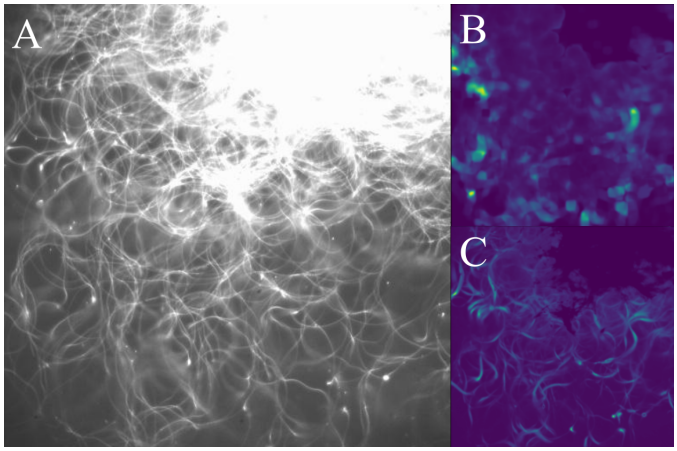

Fig. 2: (A) A real image of drosophila sperm obtained by phase contrast microscopy. Per-pixel heatmaps illustrating the change in pixel brightness over course of the video, as a measure of motility for optical flow (B) and temporal variation (C). Brighter colours indicate higher motility.

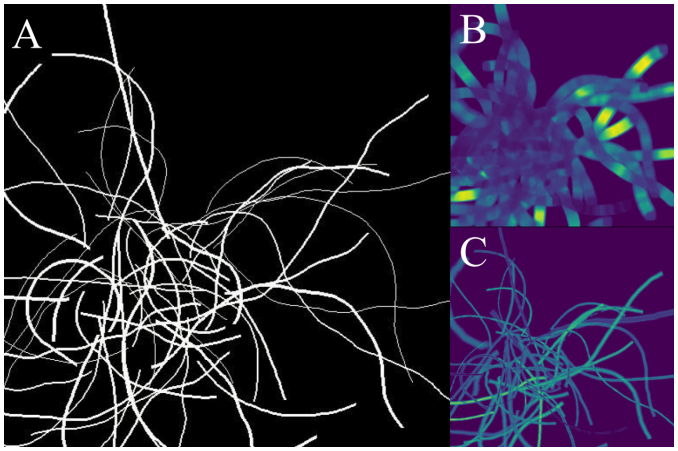

Fig. 3: A still image from a synthetic dataset mimicking drosophila sperm motion. Per-pixel heatmaps illustrating the change in pixel brightness over course of the video, as a measure of motility for optical flow (B) and temporal variation (C). Brighter colours indicate higher motility.

nearly indistinguishable, which seems to cause optical flow to fail to isolate individual velocities per pixel. Additionally, when multiple cells overlap during their motion, there is no well-defined velocity of that pixel for a given frame, which would lead to optical flow measurements being meaningless at those pixels. See Figs. 2 and 3 for examples of this. In the area where a large number of cells are clustered, optical flow outputs relatively low values even if there is a significant amount of motion.

2.2.2 Temporal Variation

Motility analysis of videos via temporal variation computes the average change in a pixel's value between frames. Similarly to optical flow analysis, the total motility is computed by averaging the temporal variation values across all pixels in all pairs of subsequent frames. With this method, motility can be expressed as:

$$M = \frac{1}{c}\sum_{i=1}^{f-1}\sum_{j=1}^{w}\sum_{k=1}^{h}\sum_{m=1}^{c}|V_{ijkm} - V_{(i+1)jkm}| \tag{2}$$

where, similar to (1),c is the number of color channels, and V_{ijkm} is the value of the m-th color channel of the pixel located at the k-th row of the j-th column of frame i.

2.3 Synthetic Data Generation

All videos were generated at 50 FPS at a resolution of 512×512 for a total of 1000 frames using the Pygame graphics library in Python. To generate the motion, individual fly sperm cells are represented as ropes on a 2D, frictionless plane. The ropes do not interact with each other. Each rope is composed of a set of discrete points used for simulating the physics of the rope, each separated by 5 pixels and evenly spaced throughout the rope. The number of ropes, and the length, direction, initial location, and initial angle of each rope are sampled from a random uniform distribution. The process to generate a rope is as follows:

procedure CREATEROPE($start, length, resolution$)
  $angle \leftarrow uniform(-\pi, \pi)$
  $bias \leftarrow uniform(-0.1, 0.1)$
  $pointAmount \leftarrow length/resolution$
  $points \leftarrow []$
  for $i \leftarrow 0, pointAmount - 1$ **do**
    if $i \neq 0$ **then**
      $prevLoc \leftarrow points[i-1]$
    else
      $prevLoc \leftarrow start$
    end if
    $angle \leftarrow angle + uniform(-0.1, 0.1) + bias$
    if $randint(0, 20) == 0$ **then**
      $bias \leftarrow uniform(-0.05, 0.05)$
    end if
    $x \leftarrow prevLoc[0] + cos(angle) * resolution$
    $y \leftarrow prevLoc[1] + sin(angle) * resolution$
    $points.add([x, y])$
  end for
  return $points$
end procedure

This process has the effect of creating a pseudo-random path for the initial state of the rope. The bias term ensures that the rope is sufficiently curvy, and is not just a straight line.

To emulate the sinusoidal movement of drosophila sperm, a time-varying force is applied to each discrete point on the rope. Within a rope, the forces at each point have a common amplitude and frequency. At each point, the forces are applied perpendicular to the rope at the point. Each rope has its own amplitude and frequency. Forces on each rope are applied as follows:

procedure APPLYFORCES($points, amplitude, frequency, frameNum$)
  $p \leftarrow 0$
  $phaseIncrement \leftarrow frequency/2$
  for $i \leftarrow 0, points.length - 1$ **do**
    $angle \leftarrow frequency * frameNum + p$
    $applyAcceleration(points, i, amplitude * sin(theta))$
    $p \leftarrow p + phaseIncrement$
  end for
end procedure

where *applyAcceleration(points i, a)* applies an acceleration of a at the i-th point of the rope perpendicular to the rope at point i. To simulate these physical effects, a variant of Störmer–Verlet integration is applied [5]. See Fig. 3 for an example.

2.4 Ground Truth Metrics

To analyze the accuracy and robustness of optical flow and temporal variation as applied to sperm motility analysis using the synthetic data, multiple ground truth metrics are proposed. These include:

1. $M_{g1} = \frac{1}{r}\sum_{i=0}^{r-1}(amplitude_i * length_i)$
2. $M_{g2} = \frac{1}{r}\sum_{i=0}^{r-1}(frequency_i * length_i)$
3. $M_{g3} = \frac{1}{r}\sum_{i=0}^{r-1}(amplitude_i * frequency_i * length_i)$
4. $M_{g4} = \frac{1}{r}\sum_{i=0}^{r-1}\sum_{p=0}^{n_i-1} D_{ip}$

where M_g is ground-truth motility, r is the total number of ropes, $amplitude_i$ and $frequency_i$ are the amplitude and frequency of oscillation for the i-th rope, and $length_i$ is the length in pixels of the i-th

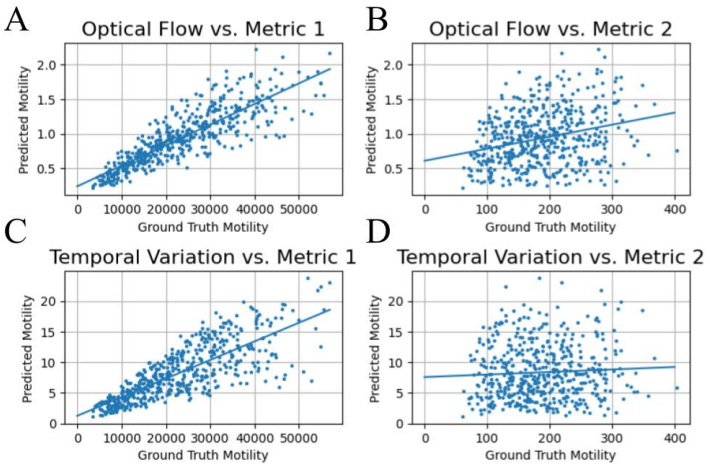

Fig. 4: Scatter plots of true and predicted motility for various analysis methods and ground truth metrics. A) Optical flow results compared to ground truth metric 1. B) Optical flow results compared to ground truth metric 2. C) Temporal variation results compared to ground truth metric 1. D) Temporal variation results compared to ground truth metric 2. Both the x and y axes are relative. Each point represents a video from the synthetic dataset. Both metrics are significantly more sensitive to amplitude than to frequency of oscillation. The fitting lines represent linear regression.

rope. D_{ip} is the total distance travelled (in pixels) by the p-th point on the i-th rope, and n_i is the total number of points in the i-th rope.

2.4.1 Limitations

1. None of the ground truth metrics account for the discrete nature of pixels. Internally, the positions of the points for each rope are represented as floating point values. These get rounded to integer values when displaying the ropes. For example, this means that if a point on a rope moves from 33.2 to 33.4, in the video it will appear as if it has not moved.
2. Neither of the metrics account for ropes which go off the screen. Due to the nature of the algorithm used to draw the initial path of the ropes, ropes may leave the screen, which is not accounted for in the ground truth metrics.

3 Results

The outputs for optical flow and temporal variation are highly correlated with each other, with $r = 0.8588$. Both optical flow and temporal variation are significantly more sensitive to amplitude than to frequency, as shown in Fig. 4 and Table 1. While optical flow is more accurate for the oscillation-based metrics (based on amplitude/frequency), temporal variation is much more accurate when using the total distance travelled by the points on the rope as the ground truth. This is likely due to the nature of optical flow and temporal variation. While optical flow is able to quantify the velocity of cell motion, temporal variation indirectly measures distance travelled by individual points in the cells by analyzing the frequency which the cell moves through a given pixel.

Overall, both temporal variation and optical flow are promising methods for analyzing the challenging visual motion of fly sperm motility.

4 Conclusion

In this preliminary work, we compare the suitability of using temporal variation and optical flow for the quantitative motility analysis of model organism *Drosophila melanogaster*. To simplify the sample data, we generate a synthetic data set that allows comparison of the methods and their performance regarding assessing differences in videos such as cell number, frequency and amplitude, without accounting for other artefacts found in real videos. We propose a new synthetic data set that closely imitates the bundling and crawling motions that makes motility measurement visually challenging. Furthermore, we design new metrics for the ground truth motility of our synthetic data set and benchmark unsupervised motion tracking methods on our data set. We conclude that both temporal variation and optical flow are relatively robust and accurate metrics for quantifying sperm cell motility.

Table 1: Correlations (r^2 values) between analysis methods and ground truth metrics on synthetic data. For oscillation-based ground truth metrics, optical flow tends to be superior, but temporal variation is more accurate when considering distance travelled by points on the cells.

Method	Ground Truth Metric			
	Amplitude	Frequency	Amplitude & Frequency	Distance
Optical Flow	0.8555	0.2764	0.8675	0.8439
Temporal Variation	0.7827	0.0588	0.6613	0.9823

As sperm cells are one of the most diverse cell types, and sperm cell analysis has not been standardized for many species, the presented methods have the potential to be applied to various other species as well that have been challenging to quantify with conventional computer-assisted sperm analysis. Further, these methods could be used to quantify other biological motility patterns as well, such as molecular motors, e.g. microtubuli that display train like patterns observed under fluorescent microscopy, and parasite or worm motion patterns in high density.

Additionally, more work needs to be done to evaluate the effectiveness of both metrics with real-world data. Non-idealities in real-world videos such as blurriness, debris and compression artifacts are not included in the synthetic data set. To further improve realism of the synthetically generated videos, techniques such as neural style transfer [6] can be applied.

Although it would be ideal to analyze the accuracy of both metrics on real videos, we can only quantitatively evaluate the accuracy of the two metrics with the artificial videos. With the artificial videos, we can exactly control all the parameters used to generate them and create quantitative ground truths of motility for those videos based on the parameters. A further qualitative analysis of both metrics on real data is warranted to determine how transferable our conclusions about both motility metrics are to real-world videos. Overall, temporal variation and optical flow hold potential as powerful tools to evaluate challenging motility data sets given further development.

Acknowledgments

Veronika Magdanz thanks the TUDAZ group at TU Dresden, Germany, for providing lab space, equipment and fruit flies for video recording of the sperm cells.

References

[1] S. Pitnick, D. J. Hosken, and T. R. Birkhead, “Sperm morphological diversity,” *Sperm biology*, pp. 69–149, 2009.

[2] Y. Heifetz and P. K. Rivlin, “Beyond the mouse model: using drosophila as a model for sperm interaction with the female reproductive tract,” *Theriogenology*, vol. 73, pp. 723–739, 2010. [Online]. Available: internal-pdf://185.59.96.8/HeifetzTheriogenologySpermstorageAntioxidants.pdf

[3] Y. Yang and X. Lu, “Drosophila sperm motility in the reproductive tract,” *Biology of Reproduction*, vol. 84, pp. 1005–1015, 2011. [Online]. Available: internal-pdf://140.98.13.172/Yang&Lu2011.pdf

[4] G. Farnebäck, “Two-frame motion estimation based on polynomial expansion,” in *Image Analysis: 13th Scandinavian Conference,*

SCIA 2003 Halmstad, Sweden, June 29–July 2, 2003 Proceedings 13. Springer, 2003, pp. 363–370.

[5] E. Hairer, C. Lubich, and G. Wanner, "Geometric numerical integration illustrated by the störmer–verlet method," *Acta numerica*, vol. 12, pp. 399–450, 2003.

[6] H. Huang, H. Wang, W. Luo, L. Ma, W. Jiang, X. Zhu, Z. Li, and W. Liu, "Real-time neural style transfer for videos," in *Proceedings of the IEEE conference on computer vision and pattern recognition*, 2017, pp. 783–791.